Progress In Electromagnetics Research Letters, Vol. 101, 55–62, 2021

A Miniaturised Negative Group Delay Triple Pass Band Filter Using Half Wavelength Meander Step Impedance Resonator

Anirban Neogi[1, 2, *] and Jyoti R. Panda[2]

Abstract—A Negative Group delay (NGD) triple passband filter with a lossy Meander Step Impedance Resonator (MSIR) is introduced in this article. The size miniaturization technique by increasing the number of meander turns is presented. In the process of filter design, the calculation of the total inductance value of the meander section is discussed in a simplified way. At the same time, the electrical and physical lengths of each section of meander resonator are calculated. The proposed filter has three passbands at 2.4, 5.0, and 7.4 GHz. The Group Delay (GD) in the three passbands is −2.5 ns, −2.1 ns, and −2.0 ns respectively. The more the number of meander turns is, the more the NGD will be. The proposed design is well equipped to be used in feed-forward and feed-back power amplifier applications. The frequency response exhibits satisfactory Return Losses (RLs) of −24, −25, and −22 dB at these three passbands. Four Transmission Zeros are generated at 3.35, 3.98, 6.2, and 8.31 GHz using an absorptive Folded SIR (FSIR) structure which improves the stopband performances. The overall dimension of the filter is (20.7×12) mm $= (0.16 \times 0.09)\lambda_g$.

1. INTRODUCTION

Multiband filters with good passband and stopband characteristics are in good demand for modern communication systems. Besides these evaluation characteristics, size miniaturisation is also an important issue. Group Delay (GD) is another important property which has been mostly ignored for many years. Conventional Band Pass Filter (BPF) or multiband BPF generally provides positive GD. In recent time Negative Group Delay (NGD) microwave filters have attracted much attention because of their practical and potential applications in a variety of microwave systems.

The literature survey starts with [1, 2] where the generation of NGD is explained in terms of coupling nature of parallel coupled lines. The measurement of Coupling Factor (k) and Quality Factor (Q) is mathematically analyzed. The transmission type NGD circuit is proposed in [3], which represents BPF action with good Insertion Loss and excellent reflection coefficient. The expected NGD value is realized by the finite tuning of coupling coefficient of the resonator with main transmission line. In [4], a unique method of NGD realization is proposed by means of Signal Interference Technique (SIT). The proposed method does not require any extra matching network for the purpose. The process of increasing the efficiency of the feed-forward power amplifier by the NGD circuit is proposed in [5]. Apart from this, the NGD circuit is also used to broaden the bandwidth of such amplifiers. The NGD circuit must follow a BPF before it, which is used to cancel unwanted frequency of oscillations. If an NGD circuit with BPF characteristics is proposed, the size of these amplifiers will be small. In this way, the design of a BPF with NGD characteristic finds its practical application in improving the performance of microwave systems. An NGD band-stop filter is proposed in [6], which generates NGD in stopband, but these filters cannot be used to enhance the characteristics of feed-forward and feed-back power amplifiers.

Received 21 September 2021, Accepted 27 November 2021, Scheduled 3 December 2021

* Corresponding author: Anirban Neogi (anirban07.neogi@gmail.com).

[1] Supreme Knowledge Foundation Group of Institution, Hooghly, West Bengal 721139, India. [2] School of Electronics Engineering, Kalinga Institute of Industrial Technology, (Deemed to be University), Bhubaneswar, Odisha 751024, India.

One adaptive multiband NGD RF circuit is introduced in [7], which depicts the reflectionless characteristics. The RF circuit consists of a two-stage-in-series-cascade dual-band NGD circuit which generates the conception of multi-functional passive components with NGD characteristics.

A few other aspects like efficiency improvement in cross cancellation power amplifier [8], wide band power divider [9], branch line hybrid coupler with NGD circuits [10], etc. have been reported in recent times. In each article, the resonator structure proposed must be lossy in nature to validate the NGD. Such lossy resonators are getting attentions recently for their ability to improve efficiency, enhance bandwidth, and minimize beam squint.

In this paper, we have proposed one tri-band filter with NGD at each passband which can be used well in power amplifier applications. The filter is proposed with a well-known Meander Step Impedance Resonator (MSIR) structure. The total inductance of the meander section is calculated in simplified way, and it is proved that as the number of meander turns is increased, the filter becomes more inductive, i.e., lossy, so NGD increases. Because of NGD, the Insertion Loss (IL) response of the filter was not good. But with the proper adjustment of the characteristic impedance of meander section IL is improved noticeably. The fabrication of the filter is done with Arlon AD250 of dielectric constant 2.5 and height 0.76 mm. The fabricated prototype performs well in accordance with the simulation results done with HFSS (High-Frequency Structure Simulator) 13.

2. CHRONOLOGICAL DEVELOPMENT OF THE PROPOSED FILTER

2.1. The Half Wavelength MSIR

The resonating condition for the conventional SIR structure as shown in Figure 1(a) is given by Equation (1) [16], where θ (θ_0 & θ_1) and Z (Z_0 & Z_1) represent the electrical length and impedance of each section, and K is the impedance ratio ($\frac{Z_0}{Z_1}$). The choice of K is important for the exact positioning of the resonant frequencies. Due to exact Input-Output (I/P-O/P) port impedance matching, W_0 (i.e., Z_0) is to be unchanged, and W_1 is to be varied to control K.

$$K = \tan\theta_0 \tan\theta_1 = \frac{Z_0}{Z_1} \tag{1}$$

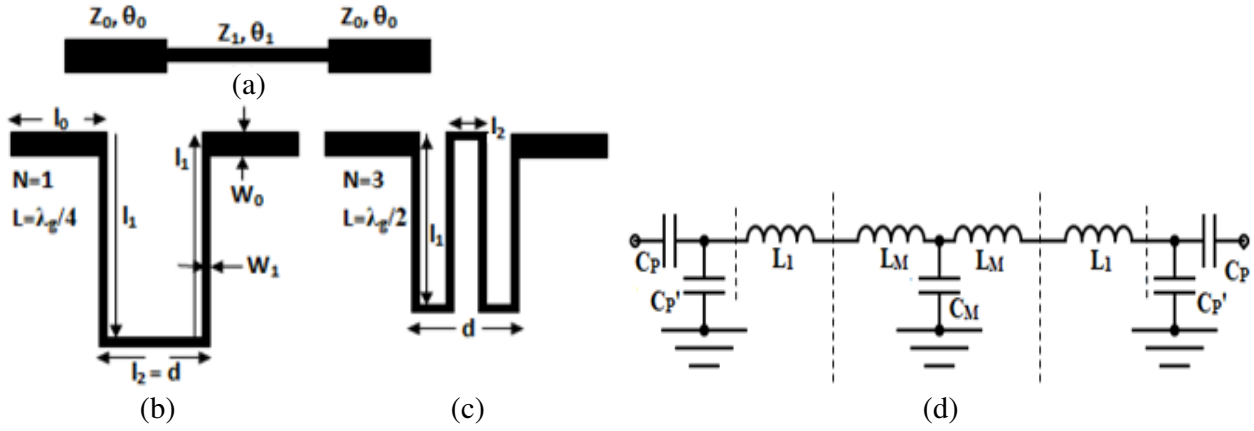

Figure 1. (a) Conventional SIR, (b) MSIR with meander turn $N = 1$, (c) MSIR with $N = 3$, (d) functional circuit.

The conventional SIR can be modified to Meander Step Impedance Resonator (MSIR) by increasing the length of the high impedance section of the SIR and folding it back. Figure 1(b) shows the MSIR structure with one meander turn ($N = 1$). It is obvious to mention that with the introduction of meander structure, the overall resonator length is increased keeping the width (d) unchanged. With reference to Figure 1(b), if the length of the high impedance section of the proposed MSIR is further increased and adjusted within the same dimensions along X axis, the number of meander turns (N)

needs to be increased. Figure 1(c) depicts the structure with $N = 3$ and the overall length of the resonator extended towards $\lambda_g/2$ (where λ_g is the guided wavelength at the first resonant frequency). Upon proper adjustment of all the dimensions and appropriate I/P and O/P coupling, the $\lambda_g/2$ resonator generates three resonating modes. From Figures 1(b) and (c) it is obvious that the value of l_2 decreases with increasing N. Here in Figure 1(c), $d = 3l_2$ and the overall length of MSIR can be expressed as

$$2l_0 + (N+1)l_1 + Nl_2 = \lambda g/2 \tag{2}$$

Equation (2) is basically a generelised equation for $\lambda g/2$ MSIR with any number of meander turn value N. As N increases, the gap between the meander lines (l_2) decreases. For the resonator shown in 1(c), $W_1 = 0.3\,\text{mm}$, $W_0 = 0.6\,\text{mm}$, and substrate height is $h = 0.8\,\text{mm}$ with relative permittivity of the substrate $\varepsilon_r = 2.5$, the characteristic impedance and effective permittivity of all the sections can be calculated as [16],

$$Z_c = \frac{\eta}{2\pi\sqrt{\varepsilon_{reff}}} \ln\left[8\frac{h}{W} + 0.25\frac{W}{h}\right] \tag{3}$$

$$\varepsilon_{reff} = \frac{\varepsilon_r + 1}{2} + \frac{\varepsilon_r - 1}{2}\left\{\left(1 + 12\frac{h}{W}\right)^{-0.5} + 0.04\left(1 - \frac{W}{h}\right)^2\right\} \tag{4}$$

Here W is the width, and Z_c is the characteristic impedance of any generalised microstrip line. From Eqs. (3) and (4), characteristic impedance and effective relative permittivity (ε_{reff}) of each section of the proposed resonator can be calculated. With increasing value on N, the effect of mutual inductance plays a more important role in calculating the total MSIR inductance. The inductive behavior of MSIR structures is well explained and mathematically presented in [15, 17]. The total inductance of the MSIR is the sum of self-inductances of all segments and the negative and positive mutual inductances between all meander lines.

$$\begin{aligned} L_T &= (L_{\text{self}})_{\text{Total}} \pm (L_m)_{\text{Total}} \\ &= (L_{\text{self-0}} + L_{\text{self-1}} + L_{\text{self-2}}) \pm (L_m)_T \qquad (5) \\ &= \left\{\left(2l_0\frac{Z_{c0}}{C}\right)\sqrt{\varepsilon_{reff}} + \left(2l_1\frac{Z_{c1}}{C}\right)\sqrt{\varepsilon_{reff}} + \left(l_2\frac{Z_{c2}}{C}\right)\sqrt{\varepsilon_{reff}}\right\} \pm (L_m)_T \qquad (6) \end{aligned}$$

where $L_{\text{self-0}}$, $L_{\text{self-1}}$, and $L_{\text{self-2}}$ represent the self inductances of the l_0, l_1 section, and l_2 sections, respectively. All these self inductances can be calculated upon calculation of Z_c and ε_{reff} of corresponding l_0, l_1, and l_2 sections as shown in Eq. (6). $(L_m)_T$ represents the mutual inductance of meander line sections of length l_1, width W_1, and separated by the gap $(l_2 - 2W_1)$. Therefore, $(L_m)_T$ will be effectively the function of l_1 and $(l_2 - 2W_1)$ [15]. Hence, $(L_m)_T$ may be concluded through Equation (7).

$$(L_m)_T = \pm\frac{\mu_0}{2\pi}l_1\left[\ln\left\{\frac{l_1}{l_2 - 2W_1} + \sqrt{1 + \left(\frac{l_1}{l_2 - 2W_1}\right)^2}\right\} - \sqrt{1 + \left(\frac{l_2 - 2W_1}{l_1}\right)^2} + \frac{l_2 - 2W_1}{l_1}\right] \tag{7}$$

It has already been mentioned that $(L_m)_T$ will be the function of l_1 and $(l_2 - 2W_1)$. Increasing the number of meander turns (N) will reduce the value $(l_2 - 2W_1)$. This in turn, as per Equation (7), will increase the value of $(Lm)_T$. So with increasing meander turn (N), the total inductance of the resonator increases which in turn will make it lossy. As a result, the Group Delay at three resonant frequencies will be negative. NGD at three passbands will surely degrade the IL performance. To avoid this, a perfect I/P-O/P matching with the resonator is essential which can be done through increasing the characteristics impedance of θ_0 and θ_1 sections, i.e., Z_{C0} and Z_{C1} [16]. The functional circuit of the MSIR is shown in Figure 1(d). L_1 corresponds to self inductance of line section l_0, l_1 and l_2. L_M and C_M represent equivalent meander mutual inductance and interdigital capacitance. As the value of N increases, L_M changes accordingly. C_P and C'_P represent the coupling capacitances at input and output ports. It has already been mentioned that the resonator of Figure 1(c) generates three resonating frequencies. At all three resonance conditions, the overall capacitance of the resonator is calculated from Eq. (9), where f is the resonating frequency and L_T found from Eq. (7).

$$C = \frac{1}{L_T(2\pi f)^2} \tag{8}$$

When the resonator of Figure 1(c) is properly coupled at input and output ports, it develops a tri-band filter with three resonating centre frequencies at 2.4, 5.0, and 7.4 GHz. The filter layout and its frequency response are depicted in Figures 2(a) and (b). The stopband performance of the filter is an issue in terms of unavailibility of Transmission Zeros (TZ). For this purpose, one Folded Step Impedance Resonator (FSIR) structure is accurately placed at the close vicinity of the proposed filter as shown in Figure 2(a). The added structure acts as a discharging circuit during the stopband of the filter. The FSIR structure also minimizes the effects of the harmonic passbands and has no effect on the filtering response. As discussed in [11], by choosing the impedance ratio of FSIR, four TZs can be achieved. The length l_5 has characteristic impedance 118.71 Ω, and the length section $(l_6 + l_7 + l_8)$ generates characteristic impedance 100 Ω. Therefore, the impedance ratio of the FSIR structure is 0.84, at which the best stopband performance is available. FSIR has no effects on the filtering responses except it creates four TZs in the stopbands. The minimum ILs in the three passbands are |3.5 dB|, |3.1 dB|, and |3 dB|. Because of meander turn in MSIR structure, NGDs are developed in all three passbands of values −1.6 ns, −0.9 ns, and −0.96 ns, respectively (Figure 2(c)). To design a triple band filter with passband centre frequencies at 2.4, 5, and 7.4 GHz, the specifications of the structure in Figure 2(a) are (in mm) $l_0 = 6.8$, $l_1 = 6.8$, $l_3 = 6.5$, $l_4 = 8.7$, $l_5 = 9.5$, $l_6 = 5.1$, $l_7 = 3.3$, $l_8 = 2$, $W_0 = 0.6$, $W_1 = 0.3$, $W_2 = 0.6$, $W = 2$, $d1 = 0.5$, $d = 3$, and $l_2 = 4.9$ mm, and the overall size is (20.7×14) mm $= (0.16 \times 0.11)\lambda_g$. With these design specifications, at the resonant frequency of the first passband (2.4 GHz), $(L_m)_T$ and C of the resonator circuit with $N = 3$ shown in Figure 2(a) are theoretically calculated as 3.72 nH and 1.2 pF from Equations (8) and (9). The characteristic impedance of the resonator (Figure 2(a)) is 331.2 ohm from Equation (3).

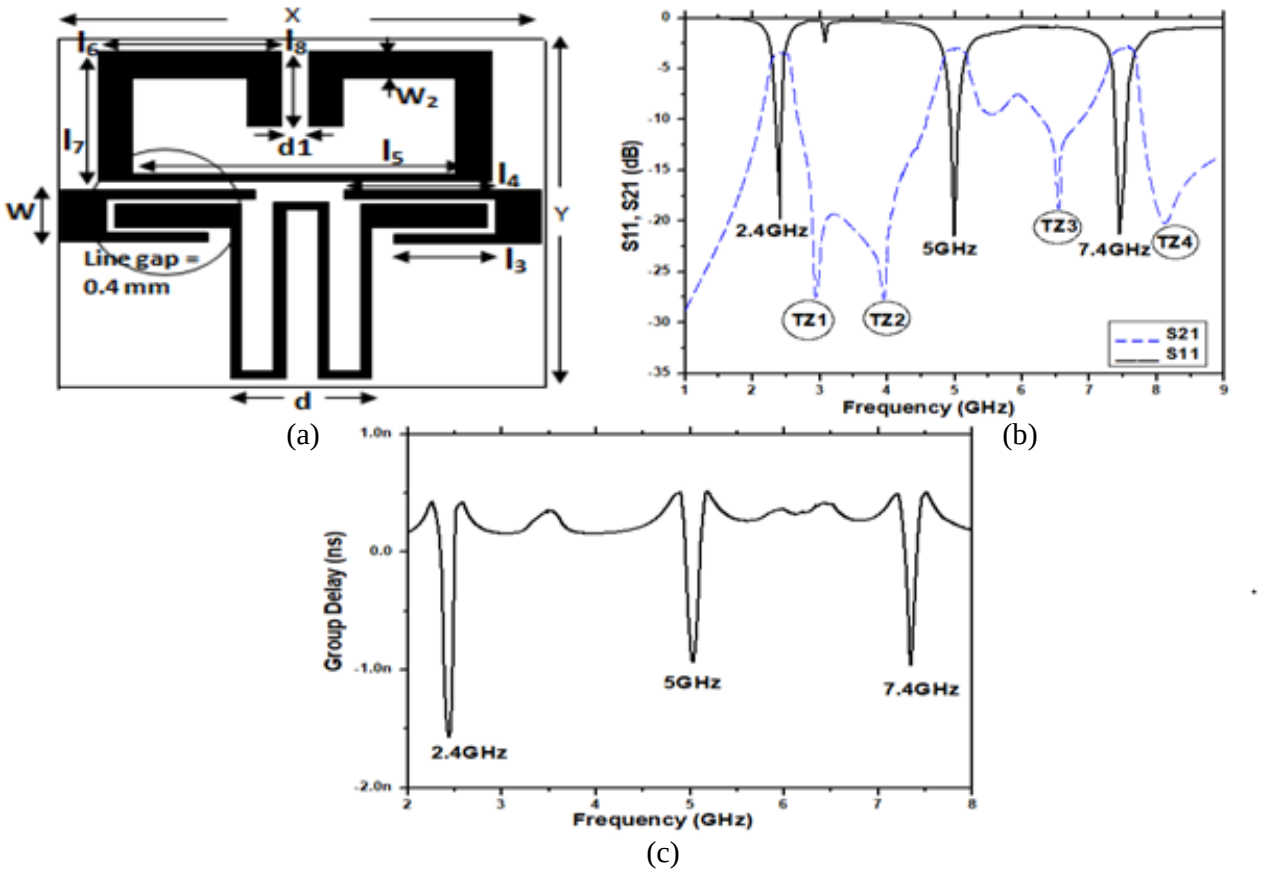

Figure 2. (a) Tri band filter using MSIR with $N = 3$, (b) and its frequency response, (c) NGD at three passbands.

2.2. The Final Filter Design

It is well discussed in Section 2.1 that, as the number of meander turns increases the filter dimension is reduced, and at the same time the resonator becomes lossy, hence the NGD and IL at three passbands will increase. To start with the final filter design, an MSIR resonator with five meander turns ($N = 5$) is proposed. A tri-band filter with passband centre frequencies at $f1 = 2.4$, $f2 = 5$, and $f3 = 7.4$ GHz is aimed to be developed. To start with, the resonator length needs to satisfy Equation (2). The proposed resonator is shown in Figure 4(a) which satisfies Equation (9).

$$2l_0 + (5+1)l_1 + 5l_2 = \lambda_g/2 \tag{9}$$

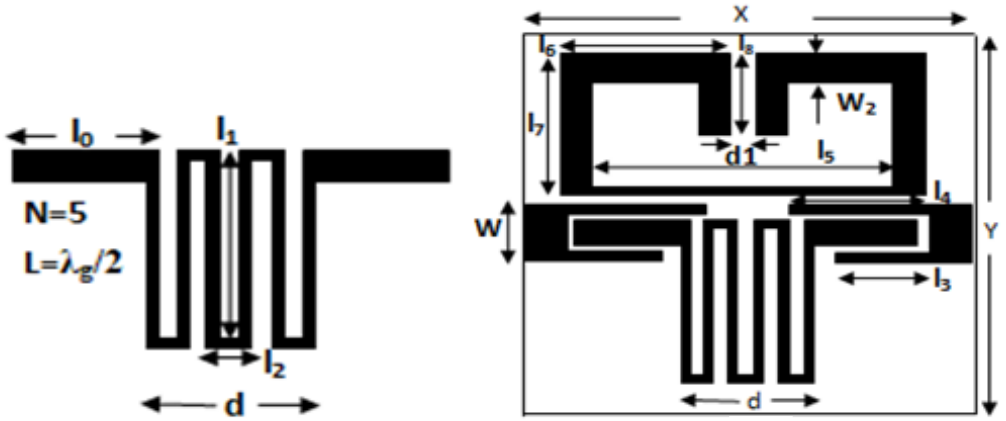

Figure 3. (a) MSIR with meander turn $N = 5$ and (b) final filter design.

The length marked with l_0 is tuned at value $l_0 = 6.8$ mm and of width 0.6 mm which is equivalent to electrical length $\theta_0 = 27.25°$ at the first resonating frequency 2.4 GHz. Similarly in the meander section $l_1 = 4.5$ mm and $l_2 = 0.98$ mm with width $W_1 = 0.3$ mm, so that the total length of the meander section is $(4.5\,\text{mm} \times 6) + (0.98\,\text{mm} \times 5) = 31.9$ mm which is equivalent to $\theta_1 = 125°$. Therefore, the total electrical length of the MSIR is 2. $\theta_0 + \theta_1 = 179.5° \sim 180°$. Now from Eqs. (4) and (5), the values of Z_c and ε_{reff} can be calculated. The electrical lengths θ_0 and θ_1 correspond to characteristic impedance $Z_{C0} = 100$ and $Z_{C1} = 130$ ohm, respectively. Since with the increasing value of N, $(L_m)_T$ increases, the characteristic impedance of $(\theta_0)l_0$ and $(\theta_1)l_1$ section is required to be increased. Such an increment of characteristic impedance will lower the IL [12]. Equation (6) may be used to calculate the total inductance of the resonator. The tri-band filter using an MSIR resonator with $N = 5$ is shown in Figure 3(b). The function of FSIR structure is already discussed, and functionally and dimectionally it remains same. The tri-band filter of Figure 3(b) generates the same response in terms of the passband centre frequency like the filter shown in Figure 3(a). Since the number of meander turns is increased, more negative group delay will be available in all three passbands. The proposed filter of Figure 3(b) has the dimension (20.7×12) mm $= (0.16 \times 0.09)\lambda_g$, so size miniaturisation is also achieved by increasing N.

3. RESULT ANALYSIS AND PARAMETRIC STUDY

Simulation of all the filters designed in this paper is done with HFSS v.13. The frequency response of the proposed filter of Figure 3(b) is presented in Figure 4(a). Centre frequencies of three passbands are 2.4, 5, and 7.4 GHz, and the passband minimum insertion losses are -5.2, -4.2, and -4.1 dB, respectively. Such low ILs irrespective of the NGD, generated at three passbands of values -2.5 ns, -2.1 ns, and -2.0 ns respectively (Figure 4(b)), are possible only due to the maximisation of the characteristic impedance of $(\theta_0)l_0$ and $(\theta_1)l_1$ sections. If the number of meander turns goes on increasing, Z_{C0} and Z_{C1} need to be increased further. The frequency response exhibits satisfactory RLs of -24, -25, and

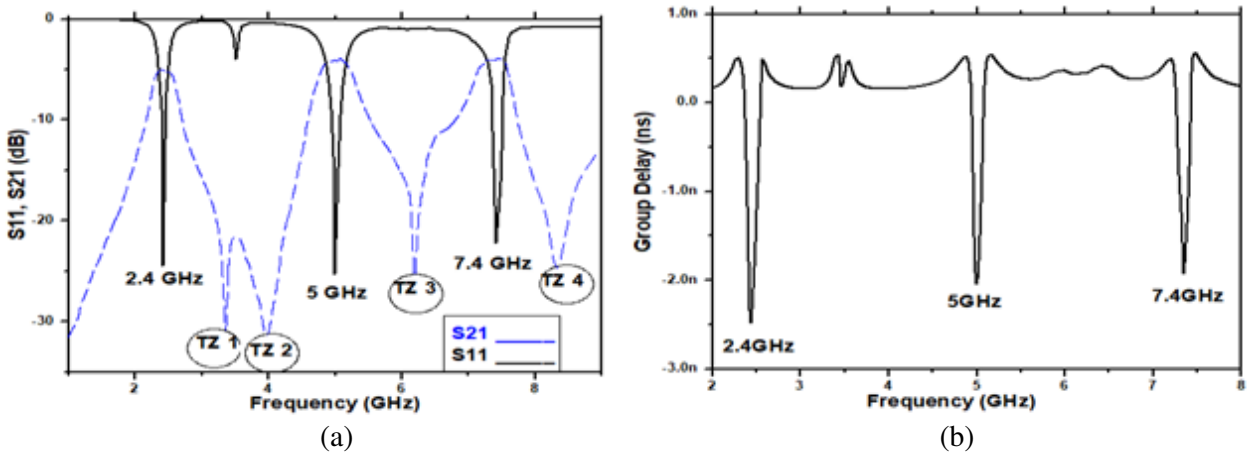

Figure 4. (a) Simulated frequency response and (b) NGD at three pass bands of the final filter with $N = 5$ Meander turns.

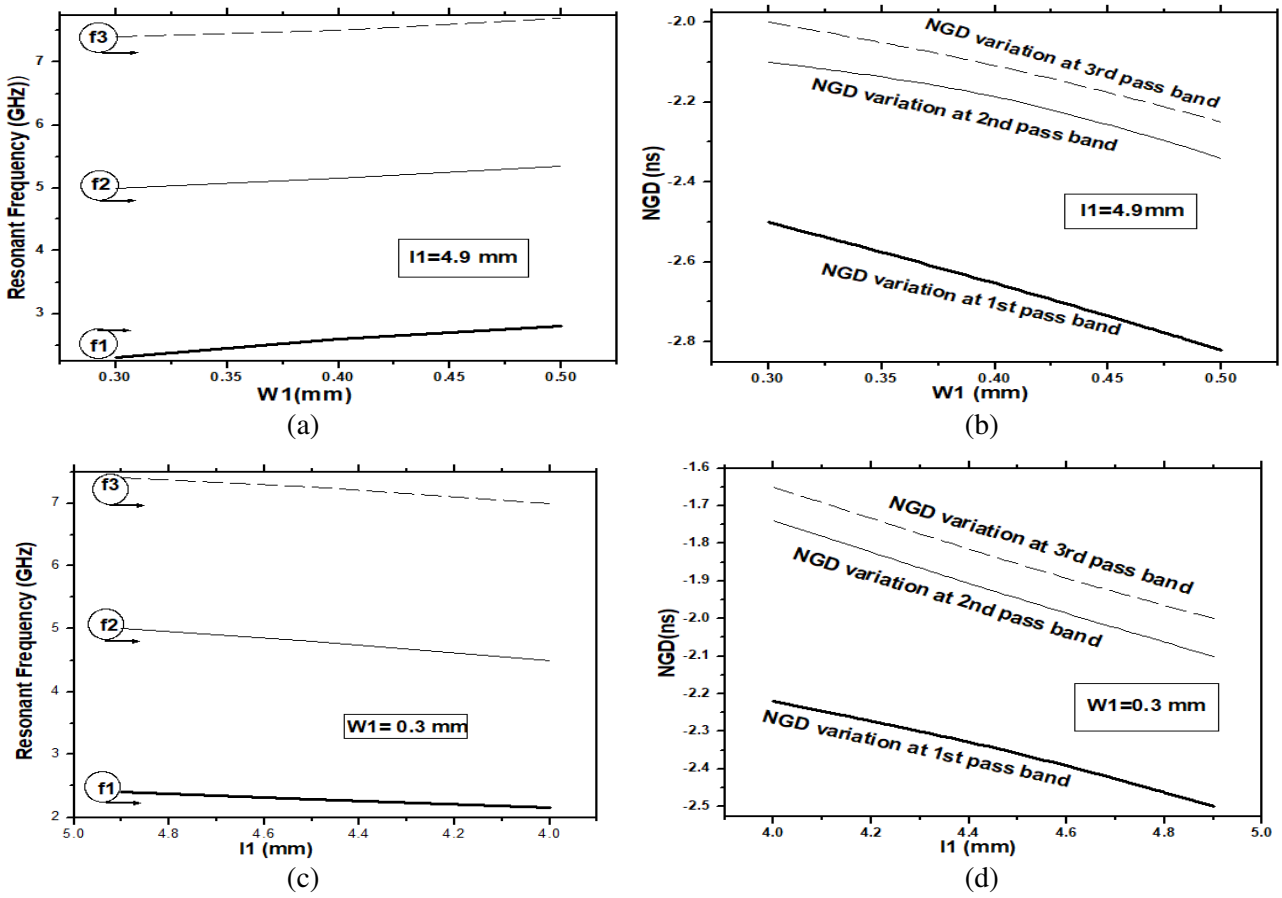

Figure 5. (a) & (b) Parametric study of centre pass band frequencies (f_1, f_2, f_3) and NGD with W_1, (c) & (d) same parametric study with l_1.

-22 dB at these three passbands. As stated earlier, the FSIR structure produces four TZs at 3.35, 3.98, 6.2, and 8.31 GHz and also suppresses the harmonic passbands which improve the stopband performance.

If we keep changing the meander line width W_1 from 0.3 to 0.6 mm, keeping l_0 and W_0 constant,

the meander impedance ratio (as well as the characteristic impedance of l_1) will keep changing. At $W_1 = 0.6\,\text{mm}$, the MSIR is converted into a Meander Uniform Impedance Resonator (MUIR). The impedance ratio (K) as defined in Equation (1) increases with increasing value of W_1, and with increasing value of K, the resonant frequency of three passbands increases when l_1 is kept constant at 4.9 mm (Figure 5(a)). At the same time the NGD in each passband keeps increasing (Figure 5(b)). Since we are aiming at the resonance bands of 2.4, 5, and 7.4 GHz as Figure 3(b), we choose $W_1 = 0.3\,\text{mm}$ and $K = 0.8$. Similerly with decreasing value of l_1 (keeping $W_1 = 0.3\,\text{mm}$) from 4.9 mm to 4 mm, and the total inductance of the MSIR decreases, hence NGD, as well as the passband centre frequency, will decrease as shown in Figures 5(c) & 5(d).

To validate the proposed filter design, a prototype is fabricated on a Arlon AD 250 substrate of dielectric constant 2.5 with height 0.76 mm. The prototype is shown in Figure 6. The NGDs at three passbands are are recorded to be -2.3, -1.95 and -1.86 ns. The ILs of the fabricated prototype at three passbands are -5.6, -4.4, and -4.3 dB, but the RL degrade (-11.3, -13.6, and -16.5 dB) because of the mismatch at the port end. Three passband frequencies are 2.38, 5.0, and 7.5 GHz which are almost identical to the simulated results. All the four TZs are available as in measured result. A comparative study of the proposed filter with two contemporary papers is presented in Table 1.

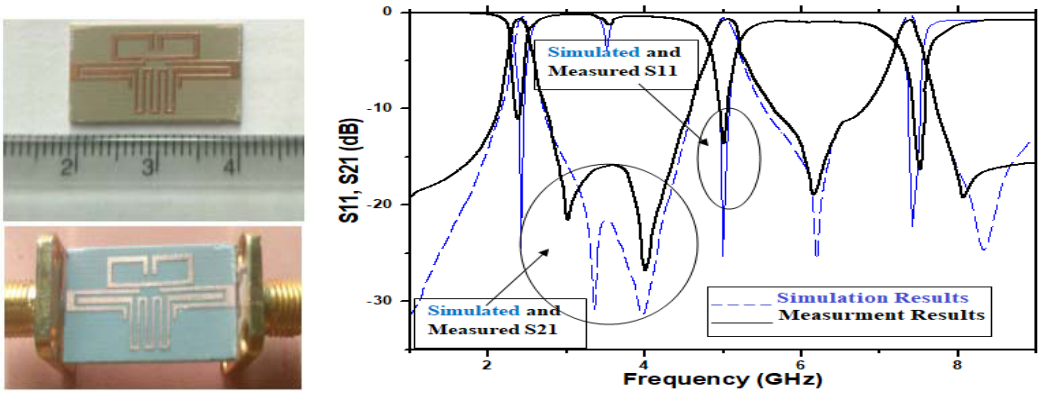

(a) (b)

Figure 6. Comparison of simulated & measured frequency response.

Table 1. Comparison of the proposed filter with some contemporary research.

Ref.	Cent. freq. (GHz)	NGD at pass band (ns)	|RL| (dB)	|IL| (dB)	$\lambda_g \times \lambda_g$
[13]	2.8, 4.3, 5.8	$-6.5, -5.4, -3$	—	21, 24, 23	0.38×0.03
[14]	1.2, 3.5, 5.8	$-1.08, -1.19, -1.09$	16.1, 17.6, 16.4	16.4, 24.6, 18.9	0.34×0.59
This work (measurement result)	2.4, 5.0, 7.4	$-2.3, -1.95, -1.86$	11.3, 13.6, 16.5	5.6, 4.4, 4.3	0.16×0.09

4. CONCLUSIONS

A triple passband filter is proposed in this paper using a $\lambda_g/2$ MSIR resonator. A methodical approach is presented to calculate the total inductance of the meander section. It is established in the paper that as the number of meander turns increases, the resonator becomes more inductive and hence lossy. The lossy resonator produces NGD in all three passbands. The more the number of meander turns is, the more the NGD will be, and this feature of the presented design enables it to be used in feed-forward

and feed-back power amplifier applications. With HFSS simulations for $N = 3$, when the NGDs at three passbands are -1.6 ns, -0.9 ns, and -0.96 ns, with $N = 5$, the values become -2.5 ns, -2.1 ns, and -2.0 ns, respectively. It is also established in the paper that the dimension of the filter is reduced by increasing the number of meander turns. A calculation of physical and electrical lengths of meander sections (namely θ_0 and θ_1) is presented here to attain the minimum possible value of Insertion Loss (IL). The proposed filter has the dimension (20.7×12) mm $= (0.16 \times 0.09)\lambda_g = 0.014\lambda_g^2$, which produces three passbands at 2.4, 5.0, and 7.4 GHz. The fabricated prototype response is in good accordance with the simulation result.

REFERENCES

1. Ravelo, B., "Theory of coupled line coupler-based negative group delay microwave circuit," *IEEE Trans. Microwave Theory Tech.*, Vol. 64, No. 11, 3604–3611, 2016.
2. Chaudhary, G. and Y. Jeong, "Negative group delay phenomenon analysis using finite unloaded quality factor resonators," *Progress In Electromagnetics Research*, Vol. 156, 55–62, 2016.
3. Liu, G. and J. Xu, "Compact transmission-type negative group delay circuit with low attenuation, *Electron. Letters*, Vol. 53, No. 7, 476–478, 2017.
4. Wang, Z., Y. Cao, T. Shao, S. Fang, and Y. Liu, "A negative group delay microwave circuit based on signal interference techniques," *IEEE Microwave Wireless Compon. Lett.*, Vol. 28, No. 4, 290–292, 2018.
5. Choi, H., Y. Jeong, C. D. Kim, and J. S. Kenney, "Efficiency enhancement of feed forward amplifiers by employing a negative group-delay circuit," *IEEE Trans. Microwave Theory Tech.*, Vol. 58, No. 5, 1116–1125, 2010.
6. Qiu, L., L. Wu, W. Yin, and J. Mao, "Absorptive band stop filter with prescribed negative group delay and bandwidth," *IEEE Microwave Wireless Compon. Lett.*, Vol. 27, No. 7, 639–641, 2017.
7. Gómez-García, R., J.-M. Muñoz-Ferreras, and D. Psychogiou, "Adaptive multi-band negative-group-delay RF circuits with low reflection," *IEEE Transactions on Circuits and Systems*, Vol. 68, No. 5, May 2021.
8. Joeng, J., G. Chaudhary, and Y. Jeong, "Efficiency enhancement of cross cancellation power amplifier using negative group delay circuit," *Microw. Opt. Technol. Lett.*, Vol. 61, No. 7, 1673–1677, 2019.
9. Yang, G., Q. Liu, S. Liu, and Y. Chang, "A compact wideband filtering power divider," *Progress In Electromagnetics Research Letters*, Vol. 81, 71–76, 2019.
10. Du, R.-N., Z.-B. Weng, and C. Zhang, "A miniaturized filtering 3-dB branch-line hybrid coupler with wide suppression band," *Progress In Electromagnetics Research Letters*, Vol. 73, 83–89, 2018.
11. Wang, Y. X., Y. L. Chen, W. H. Zou, W. C. Yang, and J. Zen, "Dual-band bandpass filter design using stub-loaded Hairpin resonator and meandering uniform impedance resonator," *Progress In Electromagnetics Research Letters*, Vol. 95, 147–153, 2021.
12. Wang, Z., Z. Fu, C. Li, S.-J. Fang, and H. Liu, "A compact negative-group-delay microstrip bandpass filter," *Progress In Electromagnetics Research Letters*, Vol. 90, 45–51, 2020.
13. Xiao, J. and Q. Wang, "Individually controllable tri-band negative group delay circuit using defected microstrip structure," *Cross Strait Quad-Regional Radio Sci. Wirel. Technol. Conf.*, 1–3, Taiyuan, China, 2019.
14. Meng, Y., Z. Wang, S.-J. Fang, and H. Liu, "A tri-band negative group delay circuit for multiband wireless applications," *Progress In Electromagnetics Research C*, Vol. 108, 159–169, 2021.
15. Grover, F. W., *Inductance Calculations, Working Formulas and Tables*, D. van Nostrand Company, Inc., Princeton, 1946; reprinted by Dover Publications, New York, 1954.
16. Makimoto, M. and S. Yamashita, *Microwave Resonators and Filters for Wireless Communication*, Springer, 2003.
17. Stojanovic, G., L. Živanov, and M. Damjanovic, "Compact form of expressions for inductance calculation of meander inductors," *Serbian Journal of Electrical Engineering*, Vol. 1, No. 3, 57–68, November 2004.